Surface Modification of Halogenated Polymers. 8. Local Reduction of Poly(tetrafluoroethylene) by the Scanning Electrochemical Microscope − Transient Investigation

Catherine Combellas,* Frédéric Kanoufi, and Driss Mazouzi

Laboratoire Environnement et Chimie Analytique, UMR 7121, 10 rue Vauquelin, 75231 Paris Cedex 05 France

Received: July 28, 2004; In Final Form: September 15, 2004

Local reduction of poly(tetrafluoroethylene) (PTFE) was achieved by scanning electrochemical microscopy (SECM). The PTFE reduction process was analyzed by the current transients, which helped propose general trends for PTFE microfabrication. The SECM was used to investigate quantitatively the kinetics of PTFE phase transformation. In a short time, a nucleation process accounts for the PTFE reduction evolution. The nucleation rate follows a potential dependency similar to that observed for conducting polymer growth or metal deposition. At long time, the expansion of the PTFE carbonization proceeds in a hemi-ellipsoidal fashion, the radial expansion being much easier than the in-depth one. Those expansions can be correlated to the tip current when changing reduction time, reducing species concentration, nature of the electrolytic solution, SECM tip radius, and tip−substrate separation. The stoichiometry of the reduction was estimated, and the existence of two kinetic regimes owing to the redox mediator reduction potential was evidenced, which confirmed previous results by feedback experiments. A rough model was proposed in which the reduction along the in-depth direction is mainly controlled by a diffusive process while the material resistivity controls the radial expansion. The observed variations may be explained by penetration of the reducing species into the rough reduced PTFE material.

1. Introduction

Fluoropolymers are widely used in applications where their low degree of chemical activity, their high-temperature resistance, their low dielectric constant, and their low frictional resistance make them prime choices in chemical, electrical or mechanical systems.[1,2] However, as a counterpart of these remarkable properties, their bonding ability is rather low, and therefore, they cannot be used just as they are, for any applications that require a good bonding ability to other materials, for example, adhesive bonding, lamination, painting, printing, and metallization. Therefore, surface pretreatment, which modifies the superficial properties of the polymer without altering bulk properties to any significant extent, has to be performed prior to using it.

Different types of treatments that are commonly used deserve mention, among which are those proceeding by photochemistry,[3] γ irradiation, ion introduction,[4] and reduction.[5−16] Reductive heterogeneous treatments have been carried out: (i) at the interface between the polymer and an amalgam of alkali metals[16−19] or (ii) at a metallic electrode located at the contact of the polymer.[20−24] Reductive homogeneous treatments are generally achieved by alkali metals dissolved in liquid ammonia[25−27] or radical-anions in the presence of alkali cations in an organic solvent.[10,28] The reductive reagent can be generated either chemically in the whole solution, electrochemically in the vicinity of the polymer via a cathode,[29] using a band ultramicroelectrode mounted on the same plane as the polymeric surface,[30] or via scanning electrochemical microscopy.[31,32] Milder reactants such as the benzoin dianion, which has to be reacted for several hours to obtain carbonization,[6,33] and magnesium solutions in liquid ammonia, which are sufficiently reactive to alter the polymeric surface structure while avoiding any noticeable carbonization,[25,34,35] may also be mentioned.

Herein we have used poly(tetrafluoroethylene) (PTFE) as the fluoropolymer because of its numerous uses. We have modified it by a radical-anion obtained in the vicinity of the microelectrode of a scanning electrochemical microscope (SECM). This method was described in a recent paper,[31] in which we have shown that fluoropolymers were easily reduced by the SECM in the feedback mode. Reduction was achieved by an electrogenerated radical-anion, $P^{\bullet -}$ ($P + e^- \rightarrow P^{\bullet -}$). It proceeds in two steps corresponding to the carbonization of the polymer

$$-(CF_2-)_n + nm\ P^{\bullet -} + n(m-2)\ H^+ \rightarrow -(CH_{m-2}-)_n + 2n\ F^- + nm\ P$$

where m was assumed to be 2, followed by doping of the carbonaceous material

$$-(CH_{m-2}-)_n + n\delta\ P^{\bullet -} + n\delta\ NBu_4^+ \rightarrow -(CH_{m-2}{}^{\delta -}-, \delta\ NBu_4^+)_n + n\delta\ P$$

The general procedure for PTFE modification is described in Scheme 1.

The approach curves indicate the presence of a time-dependent phenomenon that we have attributed to the growth of a conductive carbonaceous material. In the present paper, we will focus on the carbonized zone and study the different parameters that intervene in its growth. We will use transient methods to analyze the carbonization process and we will describe the evolution of the material modification with time.

* To whom correspondence should be addressed.

10.1021/jp046640w CCC: $27.50
Published on Web 11/19/2004

SCHEME 1: Localized Reduction of PTFE

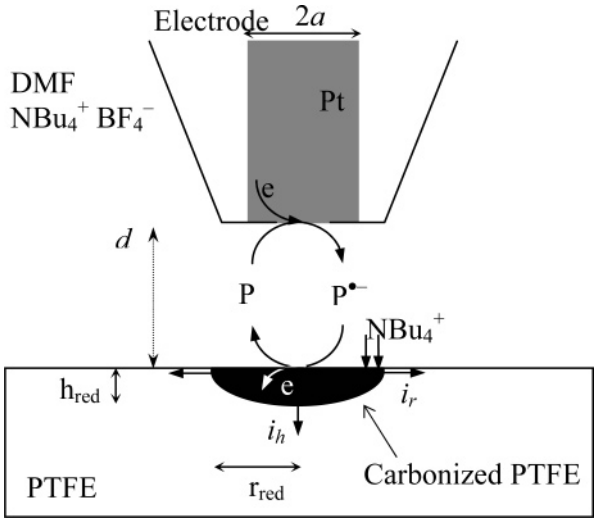

2. Experimental Section

Our experimental setup and procedures have been thoroughly described in a previous paper (see Scheme 1).[31] Typically, the electrode radius is $a = 25\ \mu$m, the distance PTFE-electrode is $d = 17\ \mu$m ($d/a = 0.68$), and the concentration of the supporting electrolyte (NBu_4BF_4) is 0.1 M. Briefly, the microelectrode was positioned at $d/a = 0.68$ by doing an approach curve toward the PTFE substrate with a redox mediator, P, such as phthalonitrile, which does not induce PTFE carbonization. The microelectrode was stopped when the tip current was 0.4 times its value at large distance from the substrate.

The water content of the electrolyte had to be carefully checked and maintained as low as possible since the size of the reduced zones decreased a lot when increasing the electrolyte water content. Indeed, water could (i) protonate the reducing agent and also (ii) add to the double bonds of reduced PTFE, which should result in the breaking of the electronic conduction path and therefore in the limitation of the radial expansion of carbonization.

PTFE samples deposited on glass by friction[36] were supplied by the "Institut Charles Sadron" (Strasbourg, France).

3. Results and Discussion

3.1. Heterogeneity of the Surface Reactivity. The typical curve for PTFE reduction at a constant tip-PTFE distance is shown in Figure 1a for 2,2′-dipyridyl as the redox mediator. It points out the lack of reproducibility in the reduction process when changing the electrode location.

Indeed, the positioning of the microelectrode was quite reproducible since it was based on the principle of negative feedback (see experimental part in ref 31), which ensures a constant tip−substrate distance.

We have attributed the dispersion of the evolution of the current to the heterogeneity of reducibility for the polymeric material. Indeed, a lateral scan of the PTFE surface with an interacting and a noninteracting reducing agent (radical anions of 2,2′-dipyridyl and phthalonitrile respectively) confirmed that the surface was smooth (estimated roughness $<1\mu$m) but spanned over a wide dispersion in reducibility (reactivity).[37]

The heterogeneity of the reactivity of the surface was emphasized when using PTFE samples deposited on glass by friction of a PTFE rod along one direction. In this case, propagation of carbonization occurred preferentially along the direction of the deposition. This shows that the intrachain propagation of charge transfer is faster than the interchain one.

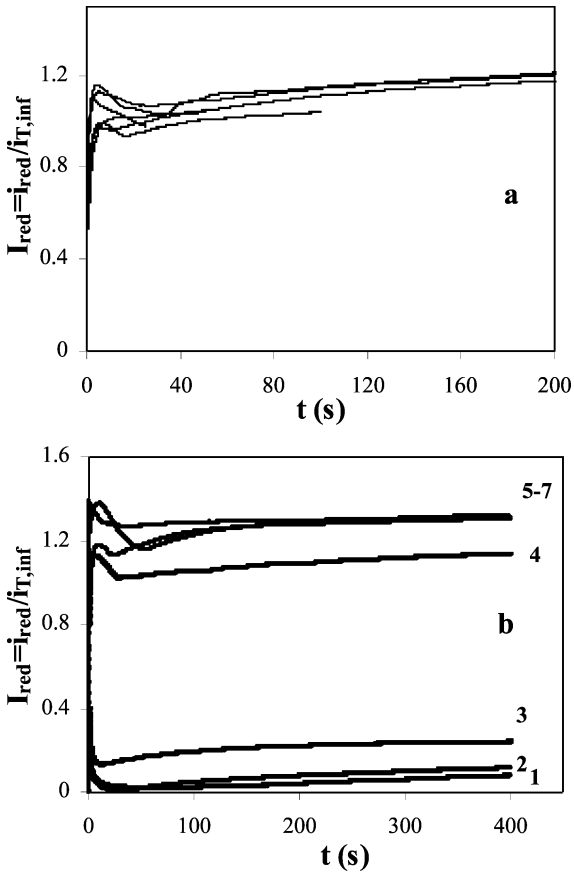

Figure 1. Chronoamperometry of PTFE reduction. Effect of the redox mediator. Distance PTFE-electrode, $d = 17\ \mu$m; electrode radius, $a = 25\ \mu$m. Supporting electrolyte: 0.1 M tetrabutylammonium tetrafluoroborate. Mediator concentration: 50 mM. Redox mediator: (a) 2,2′-dipyridyl; (b) 1, anthracene; 2, 2,4′-dipyridyl; 3, phenanthridine; 4, 2,2′-dipyridyl; 5, 4-phenylpyridine; 6, benzonitrile; 7, naphthalene.

3.2. PTFE Reduction Curves at a Constant Tip−PTFE Distance. For the sake of simplicity, we have assumed that the reduction was kinetically controlled by a first-order effective heterogeneous rate constant, k_{eff} expressed in cm s^{-1}. From the variations of the tip current due to the variations in reactivity, we have estimated the variations of the reduction rate constant. The tip current (normalized according to $i_{T,\infty}$, the value of the current at the tip placed at an infinite distance from the substrate), corresponding to such an ideal situation is given by the following set of analytical equations:[38−40]

$$I_T = I_S\,(1 - I_{T,ins}/I_{T,c}) + I_{T,ins} \qquad (1)$$

where I_S, $I_{T,ins}$, and $I_{T,c}$ are the currents normalized according to $i_{T,\infty}$, $I = i/i_{T,\infty}$ with $i_{T,\infty} = 4F[P]D_s a$ in the case of P reduction (D_S: diffusion coefficient of P in solution). They correspond to the current flowing through the substrate, the insulating tip current (diffusion controlled negative feedback), and the conductive tip current (diffusion controlled positive feedback), respectively. Their expressions as functions of the normalized distance $L = d/a$, where d is the tip−substrate distance, are given by eqs 2 and 3, respectively

$$I_{T,ins} = 1/(0.15 + 1.5358/L + 0.58\exp(-1.14/L) + 0.0908\exp[(L - 6.3)/(1.017L)]) \qquad (2)$$

$$I_{T,c} = 0.78377/L + 0.3315\exp(-1.0672/L) + 0.68 \qquad (3)$$

TABLE 1: Redox Mediators

redox mediator, P	E_P^0 (V vs SCE)[a]
phthalonitrile	−1.59
anthracene	−1.90
2,4′-dipyridyl	−1.95
phenanthridine	−2.03
2,2′-dipyridyl	−2.10
4-phenylpyridine	−2.15
benzonitrile	−2.26
naphthalene	−2.43

[a] $E°$ of the redox reaction: $P + e^- \rightarrow P^{\bullet -}$.

When the charge transfer at the substrate is controlled by an heterogeneous electron transfer of rate k_{eff}, the substrate current may be obtained from simple analytical expressions of L and k_{eff}.[38,39] We may assume that the quasi-steady PTFE reduction, observed at long-time in Figure 1, can be depicted roughly by an apparent heterogeneous electron transfer, k_{eff}. At a constant distance $d/a = 0.68$, k_{eff} is the solution of a second-order polynomial expression having I_T as a parameter. The long-time values of the curves in Figure 1 can be easily transformed to span the variability in the apparent heterogeneous reduction rate constant and demonstrate that the latter fluctuates by a factor of 2 among the different locations where the reduction proceeds.

Chronoamperograms corresponding to the evolution of the tip current placed at a constant distance to the PTFE substrate have been recorded for different redox mediators. To monitor the PTFE reduction, it is more convenient to present the data as a function of the reduction current, I_{red}, flowing through the PTFE−solution interface, rather than the tip current, I_T. Using the simple formalism developed by Mirkin, I_{red} can be deduced from I_T once the tip currents under the negative and positive purely diffusive controls, namely, $i_{T,ins}$ and $i_{T,c}$ respectively, are known. An estimate of the normalized current flowing through the substrate, $I_S = I_{red}$, is then given by (1).

As a first approximation, since $I_{T,c}$ reaches a steady current value much more rapidly than $I_{T,ins}$,[41] the variation of the substrate current with time should be the same as that for $(I_T - I_{T,ins})$. The variation of $I_{T,ins}$ with time was recorded experimentally by the use of a non interacting redox mediator such as phthalonitrile.

3.3. Qualitative Analysis of the Current−Time Response. The variation of the PTFE reduction current, I_{red}, with time is shown for different redox mediators in Figure 1b and the mediators' standard reduction potentials are gathered in Table 1. The curves depended on the redox mediator reduction strength. For all mediators, a current rise was clearly observed, after which a quasi-stationary current was reached. The time corresponding to achieve the quasi-stationary state depended on E_P^0. For $E_P^0 > -2.05$ V vs SCE, the more negative E_P^0, the faster the realization of the stationary conditions and the higher the feedback. For lower values of E_P^0 the curves were more alike and were independent of the potential.

The reduction current depicted the variation of the *n*-doped material dimensions. As will be shown later, reduced PTFE followed a radial expansion in the plane of the surface of the material with a lateral radius, r_{red}, and an elliptical expansion inside the material, $h_{red} \ll r_{red}$ (depicted in Scheme 1).

The variation of the reduction current with time relates the variations of the dimensions of the PTFE modified zone. In the following sections, we will discuss the long-time and short-time behaviors more specifically.

At long-time, the growth of the reduced PTFE zone corresponds to constant reduction current conditions. I_{red}, which is related to the extent of regeneration of P at the modified PTFE-solution interface, corresponds then merely to the charge transfer through the interface between the *n*-doped reduced PTFE and the virgin (untreated) PTFE. This charge transfer from the solution to the *n*-doped material occurs through a circular cross-talk area having a radius, r_{ct}, of the order of the tip radius, a. For feedback close to diffusion limit, as it is the case for $E_P^0 < -2.05$ V vs SCE, the electron transfer (ET) is then mainly supplied over a small disk whose radius, r_{ct}, is about $2a$.[42] We will describe the evolution of the reduced PTFE zone at long time with various experimental parameters and we will propose a model to interpret those data.

The short-time behavior is typical of a nucleation process and a rough nucleation model will be used to interpret more quantitatively the data.

3.4. Long Time Behavior. Evolution of the Material Modification. We have studied the dimensions of the modified zone as a function of different experimental parameters: time, concentration and standard reduction potential of the mediator, nature of the electrolyte, SECM tip radius, and tip−substrate separation.

3.4.1. Volume Evolution. First, we have revealed the shape of the modified zone by chemically abrading the carbonaceous reduced PTFE using strong oxidants ($NH_3/H_2O/H_2O_2$, 33/33/33, V/V/V). The abraded zone, observed by profilometry, revealed a hemi-ellipsoid of circular base. The circular base results from the radial propagation of the modification because of the cylindrical regime of diffusion provided by the tip. Radial expansion is depicted in Scheme 2 after 25 s at a distance of 1.9 a (a), 10 s (b), and 400 s (c) at a distance of 0.68 a with 2,2′-dipyridyl acting as the redox mediator. On the other hand, the elliptical profile in the $r-z$ plane is in agreement with the slower reductive flux along the z direction compared to that along the lateral one (r-axis). It is represented in Scheme 2 (d) after 400 s of reduction by the radical-anion of 2,2′-dipyridyl.

Knowledge of the modified zone dimensions (radius, r_{red}, and depth, h_{red}) and its shape helps estimate the reduction stoichiometry. The modified volume, V_{red}

$$V_{red} = (2\pi/3) r_{red}^2 h_{red} \quad (4)$$

is indeed related to the charge, Q_{red}, injected during the reduction process according to

$$Q_{red} = (m + \delta) F C_P V_{red} = (m + \delta) F C_P (2\pi/3) r_{red}^2 h_{red} \quad (5)$$

where m and δ represent the net charges injected per CF_2 unit for its reduction and its charging, C_P corresponds to the concentration of the CF_2 unit in PTFE ($C_P = 43$ M), and r_{red} and h_{red} are the radius and the width, respectively, of the ellipsoidal modification.

The injected charge, Q_{red}, can be readily deduced from the current flowing through the PTFE-solution interface, i_{red}, using

$$i_{red} = \frac{dQ_{red}}{dt} \quad (6)$$

As shown in Figure 2, we have observed a good correlation between the injected charge and the modified volume for a wide range of dimensions and charges (along 2 decades of Q_{red}). The number of electrons exchanged per monomeric unit, deduced from the slope, was equal to 3.1 for mediators with E_P^0 lower than −2.05 V. The value of 3.1 found for $m + \delta$, which is comprised between 2 and 4, indicates that one electron is exchanged per fluorine atom ($m = 2$ per CF_2 unit). It is in agreement with the general mechanism proposed for the

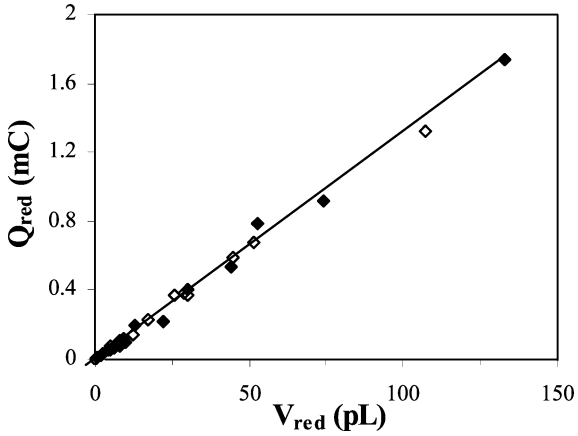

Figure 2. Variation of the charge as a function of the modified volume. ◇, 2,2′-dipyridyl: 0.005, 0.01 and 0.05 M; ◆, 4-phenylpyridine: 0.01, 0.05 M. The other experimental conditions are the same as those in Figure 1.

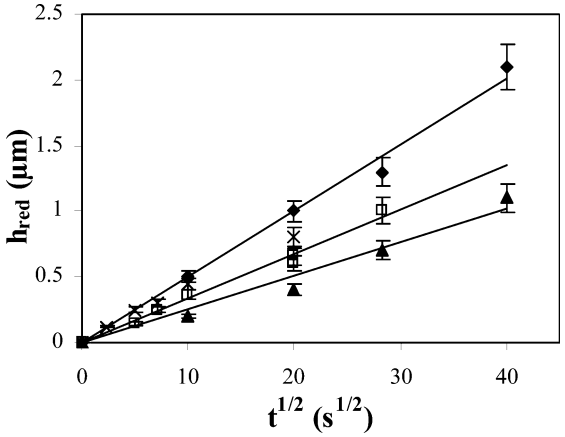

Figure 3. Variation of the depth of the carbonized zone as a function of time for different cations of the supporting electrolyte. With 2,2′-dipyridyl as mediator: ◆, tetraethylammonium; □, tetrabutylammonium; ▲, tetraoctylammonium. With 4-phenylpyridine as mediator: ×, tetrabutylammonium. The other experimental conditions are the same as those in Figure 1.

reduction of vicinal dihalogenated compounds or polyfluorinated molecules, which predicts one electron per expelled halogen atom and the formation of an olefin.[43,44] We confirm that PTFE reduction leads to the formation of a conducting polyyne structure according to[10,5,16,28]

$$-(CF_2-CF_2-) + 4\ P^{\bullet -} \rightarrow -(C\equiv C-) + 4\ F^- + 4\ P$$

The value of 1 for the charge ($\delta = 1$ per CF_2 unit) is high but in agreement with other experimental estimations.[5,30] This high value probably indicates the poor stability of the charged polymeric material. Therefore the yield for charging of the reduced PTFE material should depend on the redox mediator used for the reduction. Indeed a much higher value of $\delta \approx 4.5$ was obtained for a lesser reducing mediator such as 2,4′-dipyridyl. It indicates that under such circumstances, the PTFE reduction is slower than the discharge of the carbonaceous material.

3.4.2. In-Depth Expansion. We have observed through profilometry the variation of the depth of the modified zone with the electrolysis time and the redox mediator concentration. The variation of the depth with time is presented in Figure 3 for two different mediators and three different supporting electrolytes. We observe that h_{red} is proportional to $t^{0.5}$. It is also proportional to $[P]^{0.5}$ (not shown) and independent of the electrode radius (not shown) for the whole set of redox mediators used (whenever $E_p^0 < -2.05$ V vs SCE).

For a given time of electrolysis, the depth of the carbonized zone decreased upon increasing the size of the supporting electrolyte cation. From the slopes of the straight lines obtained on Figure 3, we have deduced the apparent diffusion coefficient, κ_h ($h_{red} = (\kappa_h t)^{0.5}$) for the different electrolytes: $\kappa_h = 25$, 14, and 6.2 10^{-12} cm^2 s^{-1} for tetra-ethyl, -butyl, and -octylammonium cations, respectively. The diffusive variations of h_{red} led to apparent carbonization rate constants of the same order of magnitude as those of the literature.[5,20]

3.4.3. Radial Expansion. Figure 4a represents the variations in the modified zone radius, r_{red}, with the reduction time for different redox mediators.

The variation of the radius of the modified zone with time and mediator concentration follows a power law such as $r_{red} \propto t^{\beta}[P]^{\beta}$ with $\beta \approx 0.25 \pm 0.02$ for the whole set of redox mediators used, as can be observed in Figure 4b. The variation of r_{red} with E_p^0 confirms that the reduction is potential independent for $E_p^0 < -2.05$ V vs SCE and less efficient for more positive values of E_p^0.

The effect of the size of the supporting electrolyte cation on the radius of the carbonized zone could be evidenced on the slopes of the straight lines obtained when representing r_{red}/a as a function of $t^{0.24\pm0.01}$ (not shown, they were equal to 1.5_5, 1.3, and 1.1 $s^{-0.24}$ for tetra-ethyl, -butyl, and -octylammonium cations, respectively). When the electrolyte cation was smaller, the radius of the carbonized zone grew faster. This effect was all the more important as the reduction time increased.

The size of the carbonized zone depended on the tip−substrate distance as can be seen in Figure 4c with 2,2′-dipyridyl acting as the redox mediator. No PTFE modification was observed even after 400 s of treatment when the electrode was further than $2-3a$ from the substrate. Actually, under such conditions, no interaction occurred between the radical-anion and the PTFE surface. Conversely, when the tip−substrate distance was less than $2a$, localized carbonization of PTFE took place. For intermediate distances ($1.5a < d < 2a$), carbonization nuclei developed within the first 20 s of reduction on an area, which was approximately the same as the diffusion layer (diameter: $2-3a$); the growing rate corresponded then to the

SCHEME 2: Radial and In-Depth Expansions

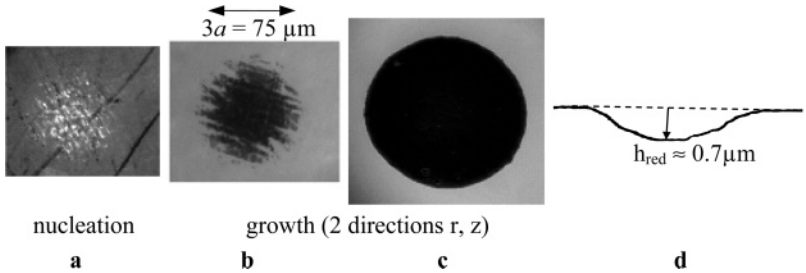

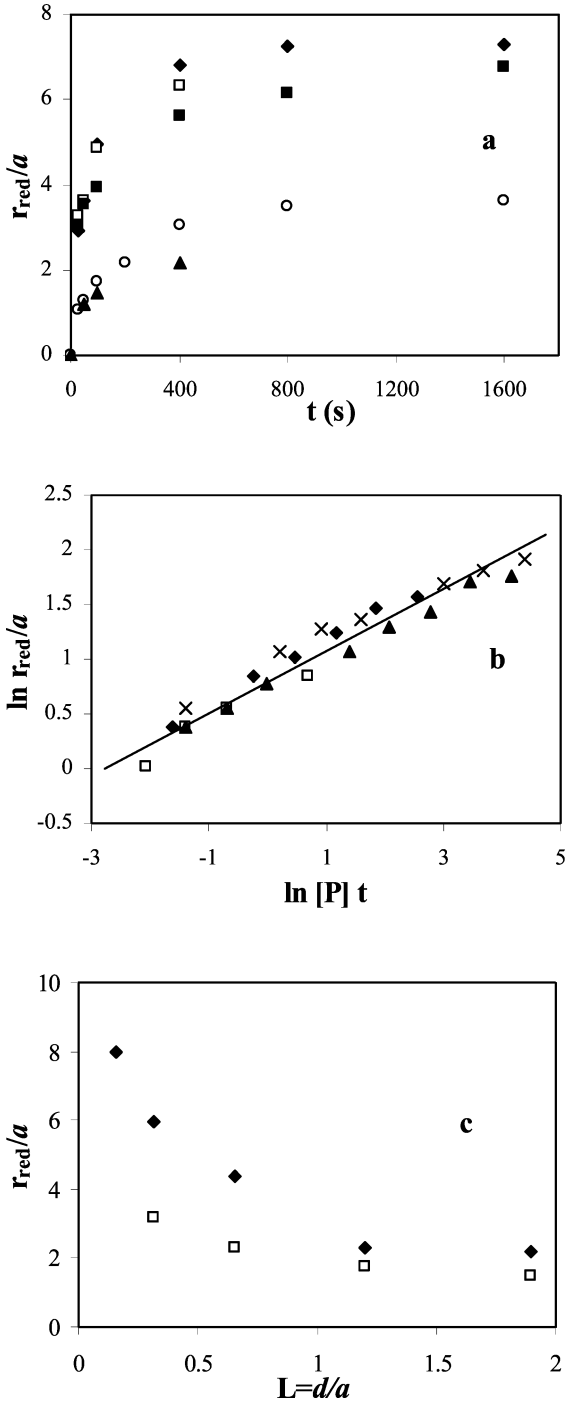

Figure 4. Radius of the carbonized zone. (a) Effect of time and redox mediator. Redox mediator: ▲, 2,4′-dipyridyl; ○, phenanthridine; ■, 2,2′-dipyridyl; □, benzonitrile; ◆, naphthalene. (b) Effect of time and mediator concentration with 2,2′-dipyridyl as mediator. Mediator concentration: ◆, 2 10^{-3} M; □, 5 10^{-3} M; ▲, 10^{-2} M; ×, 5 10^{-2} M. **c**: Effect of the electrode-substrate distance. Treatment time with 2,2′-dipyridyl as mediator: ◆, 400 s; □, 50 s. The other experimental conditions are the same as those in Figure 1.

diffusion rate of $P^{\bullet -}$ toward the PTFE surface. The slowness of the nucleation reaction could be responsible for the complexity of the approach curves described previously.[31] For short distances ($d < 0.68a$), a homogeneous carbonized disk appeared directly and no distinct nuclei were observed for times longer than 0.5 s.

The effect of the electrode size on r_{red} has also been investigated and emphasizes the influence of the material resistivity, as already stated.[30] The experiments were performed

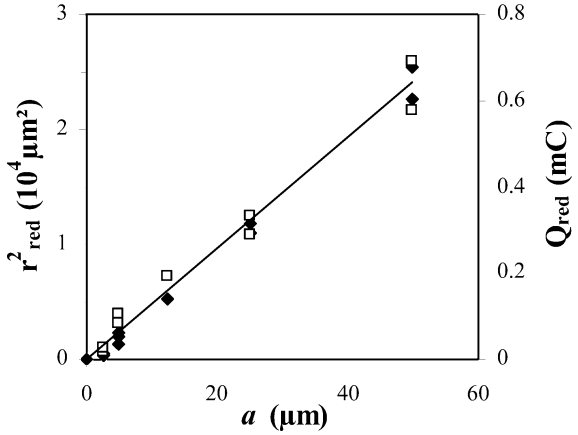

Figure 5. Variation of the square of the radius of the carbonized zone (◆) and the charge (□) as a function of the electrode radius. Same other experimental conditions as in Figure 1. Redox mediator: 2,2′-dipyridyl. $d/a = 0.68$.

at a mediator concentration of 0.05 M and a normalized tip−substrate distance of 0.68 in order to provide similar reduction current densities (Q proportional to a, as observed experimentally in Figure 5). We observed that the higher the electrode size, a, the smaller the value of r_{red}/a. Actually, r_{red}^2 varied linearly with the electrode size, a, as can be seen in Figure 5.

3.4.4. Model. We have attempted to rationalize these observations in order to explain the trends observed for the expansion of the carbonized PTFE zone. According to previous investigation with the band electrode assembly, the large current densities that flow through the electrolyte/C interface imply that the PTFE reduction occurs in the high-current regime.[30] Moreover, the time variation of the depth suggests a diffusive process for the in-depth expansion.

Let us denote i_r and i_h the current for radial and in-depth expansion, respectively. The current for lateral expansion may be written as[30,45]

$$i_r = 2\pi/3\ (2 + \delta)F\langle m_r\rangle r_{red}h_{red} = 2\pi/3\ (2 + \delta)Fk_rC_{red}r_{red}h_{red} \quad (7)$$

where r_{red} is the radius and h_{red} is the depth of the modified PTFE zone, $\langle m_r\rangle$ is the mean radial mass transfer rate of the PTFE reduction, k_r is the associated average radial heterogeneous rate constant, and C_{red} is the concentration of reducer inside the reduced PTFE. The current responsible for in-depth expansion is equal to

$$i_h = \pi/3\ (2 + \delta)F\langle m_h\rangle {r_{red}}^2 \quad (8)$$

with $\langle m_h\rangle$ the mean in-depth mass transfer rate. For large values of the reduction current, one may expect the in-depth expansion to be a diffusive process limited by ion transport into the reduced matrix[46] and i_h becomes

$$i_h = \pi/3\ (2 + \delta)FD_{red}C_{red}{r_{red}}^2/h_{red} \quad (9)$$

where D_{red} is the diffusive coefficient of the electrolyte cation in the reduced PTFE.

The elliptical shape of the PTFE modification implies that $i_r = \epsilon i_h$, where ϵ is a constant, which is expected to be equal to 1 since it characterizes the same reductive process in the two directions. However, it may change when the ohmic drop along the growing carbonized material increases.[30] The global PTFE reduction current is then $i_{red} = (1 + \epsilon)i_h$ and hence $i_{red} \propto D_{red}r_{red}^2/h_{red}$.

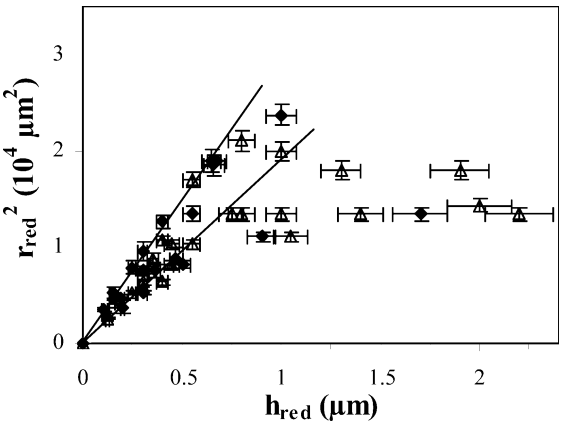

Figure 6. Variation of the square of the radius of the carbonized zone, r_{red}^2 as a function of its depth, h_{red}. Redox mediator: △, 2,2′-dipyridyl; ◆, 4-phenylpyridine. 2 mM ≤ [P] ≤ 50 mM. The other experimental conditions are the same as those in Figure 1.

The quasi-steady value for the reduction current at time $t >$ 40 s implies that i_h and i_r are constant and therefore from (7) and (9), $r_{red}^2 \propto h_{red}$ and $k_r \propto r_{red}^{-3}$, which implies that k_r is time dependent.

The diffusive limitation introduced in (9) is experimentally observed in Figure 6. The linear variation of r_{red}^2 with h_{red} is satisfied for small values of h_{red} ($h_{red} < 1$ μm). The proportionality factor is between 2.5±0.4 cm for different values of [P] and results in a constant value for

$$i_{red}/(1+\epsilon)D_{red}C_{red} = A \approx 7.5 \times 10^5 \text{ A cm} \qquad (10)$$

For larger values of h_{red}, that are measured for very large reduction time, $t >$ 600 s, the carbonized surface does not grow much, r_{red} remains constant, and ϵ increases with time. We will not further discuss this regime of nonconstant ϵ.

In the regime of constant ϵ, and at large driving force, the reduction current is close to be diffusion controlled and therefore

$$i_{red} \approx FD_s[P]\pi a^2/d = FD_s[P]\pi a/L \qquad (11)$$

with D_s the solution diffusion coefficient of the redox mediator P. The reduction current, for the given $L = d/a = 0.68$, $I_{red} = i_{red}/i_{T,\infty} \approx 1.2$, is in close agreement with the expected value of $\pi a/4d = \pi/4L = 1.1_5$ for a thin layer cell configuration[39] (see Figure 1a). The combination of (5), (6), and (9) then leads to a simple approximate time variation for h_{red} and r_{red}

$$dh_{red}^2/dt = D_{red}C_{red}(1+\epsilon)/2C_P \qquad (12)$$

$$h_{red}^2 = \frac{C_{red}(1+\epsilon)}{2C_P}D_{red}t = \kappa_h t \qquad (13)$$

$$r_{red}^4 = \frac{9D_s^2[P]^2a^2t}{2(2+\delta)^2C_P(1+\epsilon)D_{red}C_{red}L^2} = \frac{9i_{red}^2t}{4\pi^2(2+\delta)^2F^2C_P^2\kappa_h} \qquad (14)$$

According to this simple model, the experimental variations of the reduced zone dimensions with the redox mediator concentration [P] result from eq 10 as $(1+\epsilon)D_{red}C_{red}$ should be proportional to i_{red}, which is itself proportional to [P]. It implies that the concentration of the reduced charge in the reduced PTFE, C_{red}, is proportional to [P]. This would indicate partitioning or diffusion of the redox mediator into the reduced PTFE zone, which is not too unlikely owing to its important porosity. Moreover, from (10) and the values of $C_P = 43$ M and $i_{red} \approx 700$ nA for [P] = 0.05 M, we obtain, $h_{red}^2 \approx 11 \times 10^{-12}\ t$ with h_{red} in cm and t in seconds, in good agreement with the observed value of $\kappa_h = 14 \times 10^{-12}$ cm^2 s^{-1}.

Equations 13 and 14 then satisfactorily fit the observed experimental variations: $h_{red}^2 \propto r_{red}^4 \propto [P]t$. The proportionality factor between r_{red} and $t^{1/4}$ is estimated from (14) to 2.9×10^{-3} cm s$^{-1/4}$ in good agreement with the value of 3.2×10^{-3} observed experimentally. Moreover, eq 14 explains that, for a given value of L, r_{red}^2 is proportional to a, as observed in Figure 5. It also indicates that r_{red}^2 follows i_{red}, then r_{red}^2 must decrease as L increases for a given redox mediator, electrode size, and reduction time. The latter variation is also verified in Figure 4c as long as the nucleation process, occurring in a disk of radius 1.5−2 a, is completed. Finally, the observation of the potential dependency of the variation of r_{red} with time may also be explained by (14) as changing the redox mediator affects the value of i_{red}.

3.5. Short-Time Behavior. Nucleation of the PTFE Transformation. At short time, the chronoamperograms record a current rise characteristic for a nucleation process. The shape of the I−t curve obtained with, for example, 2,2′-dipyridyl shows a first peak before approaching the plateau (see Figure 1). This feature could be characteristic of a multiple nucleation process as for example those observed during multiple layer nucleation.[47] For the sake of simplicity, we have just focused on the first initial current rise. As expected for nucleation processes, during this period, the PTFE reduction occurred at different small disc-shaped sites encompassed in a disk whose radius was a few times the electrode radius. This situation is difficult to observe for small tip−substrate separations, as half the maximum current is observed for times shorter than 0.5 s. It is more easily observed when the tip is withdrawn from the substrate and typically after a 25 s reduction of PTFE by a 25 μm radius tip held at a distance $d = 1.9\ a$, one clearly observes nucleation sites as those presented on the left image of Scheme 2 (**a**). The preferential reduction of some sites is consistent with the heterogeneity of reactivity of the material described earlier. The active nucleation sites could be some micro-domains of polymer that were oriented during the polishing step, or surface irregularities such as scratches as the carbonization process is preferentially driven along those scratches. The phenomenon observed here can be related to the observation of nucleation processes at microelectrodes.[48−50] It has already been described experimentally and various theoretical models have been developed for its interpretation.[51]

We have attempted to characterize more quantitatively the nucleation process of the reduction through the cross-talk, which was established between the tip and the PTFE, by studying the variation of I_{red} with time during this initial current rise. We have mainly focused on the given tip−substrate separation of $d = 0.68a$ as it is the distance at which most data were collected. The quantification might seem odd as we have enlightened the limited reproducibility of the system. However, the kinetics of the initial current rise was reproducible and showed a clear dependency on the $E°$ of the redox mediator. We have then attempted to rationalize the nucleation process by using the model developed by Hyde et al.[52] for transport controlled nucleation as the SECM tip provides, for the given time periods ($t >$ 0.2 s), a steady-state supply of reducer. Briefly, we assume that the nucleation process is described by the general law

$$N(t) = N_0(1 - e^{-At}) \qquad (15)$$

where N is the number density of nuclei at time t, N_0 is the

saturation nucleus (the active sites) density, and A is the nucleation rate constant.

Transitory phenomena observed at times greater than the time required for the attainment of a steady-state current ($t_{lim} = d^2/D_s = 0.2$ s) can be interpreted by the nucleation process. After 0.2 s, the SECM tip is assumed to provide a steady mass transfer reduction current density, j_{red}, given by

$$j_{red} = FD_s[P]/\lambda \tag{16}$$

where λ is a constant related to the apparent interfacial ET and the tip−substrate separation. This flux is approximately linear in a disk of radius 1.5−2 times larger than the SECM tip radius, a. In this surface, the nuclei growth is then fed by planar diffusion from the tip to the PTFE surface.

We have assumed that 3D growth of a single nucleus, of radius r_n and height h_n, formed during the PTFE reduction, is controlled by a diffusive process characterizing charge transport into the reduced polymer structure. This assumption is supported through the experimental observation of the apparent diffusive expansion along the vertical axis

$$h_n(t) = (\kappa_h t)^{1/2} \tag{17}$$

with κ_h the apparent in-depth diffusive coefficient. A similar diffusive expansion along the radial axis might be observed at shorter time since the material resistance is less important than at longer time

$$r_n(t) = (\kappa_r t)^{1/2} = (\xi\kappa_h t)^{1/2} \tag{18}$$

where $\kappa_r = \xi\ \kappa_h$. As the radial expansion is faster than the vertical one, $\xi \gg 1$ and it had been estimated previously[30] of the order of 10^3.

The reduction current for a single nucleus, $i_{red,n}$, should then be given by

$$i_{red,n} = (1+\epsilon)(2+\delta)\,\pi\, FD_{red}C_{red}\, r_n{}^2(t)/(3h_n(t)) \tag{19}$$

The hemi-ellipsoidal growth of the nucleus is fed by planar diffusion of radical anion $P^{\bullet -}$ in the solution over an equivalent surface, of area $\pi r_p(t)^2$. Therefore, those two contributions may be equated for the PTFE reduction into a single nucleus

$$\pi r_p{}^2\, j_{red} = i_{red,n}$$

which leads to

$$\pi r_p{}^2 = i_{red,n}\,\lambda/D_s[P] = \lambda\,(\kappa_r' t)^{1/2} \tag{20}$$

where κ_r' has the dimension of a diffusion coefficient and

$$\kappa_r'^{1/2} = \frac{\pi(1+\epsilon)D_{red}C_{red}(2+\delta)\kappa_r}{3D_s[P]\sqrt{\kappa_h}} \tag{21}$$

The planar extended surface coverage, θ_{ex}, of N nonoverlapping nuclei ensues[49−51,53,54]

$$\theta_{ex} = \int_0^t \frac{dN}{du} S(t-u)\, du \tag{22}$$

with $S(t) = \pi r_p{}^2 = \lambda\,(\kappa_r' t)^{1/2}$. The nuclei overlapping is taken into account by application of the Avrami theorem,[55,56] which gives the real surface coverage, θ

$$\theta = 1 - \exp(-\theta_{ex}) \tag{23}$$

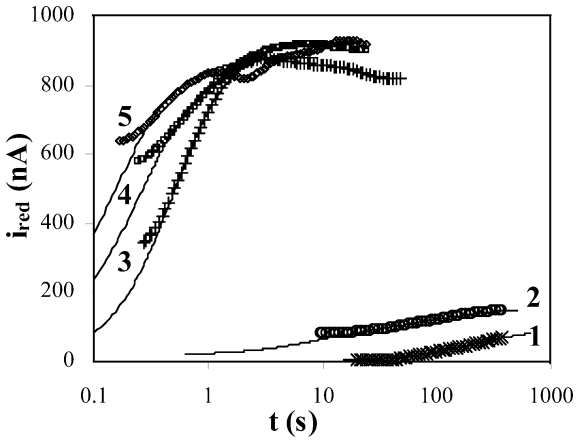

Figure 7. Chronoamperometry of PTFE reduction analyzed by the nucleation model. Same experimental condition as in Figure 1. Redox mediator: 1, 2,4′-dipyridyl; 2, phenanthridine; 3, 2,2′-dipyridyl; 4, 4-phenylpyridine; 5, benzonitrile. Symbols: experimental chronoamperograms; lines: best fit of the chronoamperograms according to (25).

The reduction current ensues

$$i_{red} = \pi(\kappa a)^2 j_{red}\,(1 - e^{-\theta_{ex}}) \tag{24}$$

where the constant κ indicates that the reduction is achieved mostly in a disk of radius κ times the tip radius, a. For a conductive substrate, the reduction current is controlled by diffusion within the tip−substrate gap. It has already been shown that the charge injection mainly occurs on the substrate on a disk area of radius,[42] $a_S = a + 1.5d$, giving here $a_S = 2a$ and $k \sim 2$. It agrees well with the dimensions of the area where the nucleation process is observed.

Hyde et al.[52] have shown that this expression may be simplified into an equation of the form

$$i_{red} = C[1 - \exp(-Bt^{1/2}\{1 - e^{-At}[1 + (At/3) + ((At)^2/10)]\})] \tag{25}$$

In this expression, A corresponds to the nucleation rate constant defined in (15), C corresponds actually to the maximum reduction current observed at longer times, $C = \pi(\kappa a)^2 j_{red}$, and $B = \lambda\kappa_r'^{1/2}N_0$ has the dimension of the square root of a rate constant characteristic of the diffusional growth of single nuclei under the SECM mass transport control.

The initial rising part of the chronoamperometric responses $i_{red} - t$ has been interpreted according to the nucleation eq 25. The values of A, B, and C obtained from the best fit of the experimental curves as presented in Figure 7 are given in Table 2. The fit is quite good for the different redox mediators in the concentration range [2−50 mM] investigated.

The low values of the nucleation rate constant, A, presented in Figure 8, suggest that the nucleation is progressive rather than instantaneous.

At high driving forces of the PTFE reduction (most negative values of E_P^0), when the latter is governed by the kinetics of charging of the reduced polymer, the nucleation becomes potential independent.

At lower driving forces, for $E_P^0 > -2.2$ V vs SCE, the nucleation of carbonized PTFE in the PTFE structure is a potential dependent phenomenon and the nucleation rate constant, A, depends on both E_P^0 and [P]. According to the atomistic theory of nucleation, it is expected that the rate of nucleation, which is related to the formation of a critical nucleus

TABLE 2: Modelization of the Current during Nucleation[a]

redox mediator, P	[P],[b] mM	*A*, s^{-1}	*B*, $s^{-1/2}$	*C*, μA
anthracene	50	0.008	0.03	0.08
2,4′-dipyridyl	50	0.02	0.04	0.1_1
phenanthridine	50	0.3_5	0.1_6	0.1_6
2,2′-dipyridyl	50	$2._2$	$2._3$	0.7
	10	$1._5$	$1._2$	0.1_6
	5	0.8	0.7	0.09
	2	0.7	0.8	0.04
4-phenylpyridine	50	8	$2._1$	0.9
	10	5	$1._3$	0.1_8
	5	3	1	0.09
benzonitrile	50	10	$2._8$	0.7_5
naphthalene	50	9	$2._5$	0.8

[a] Fit parameters of eq 25. [b] At 20 °C in DMF + 0.1 M NBu_4BF_4.

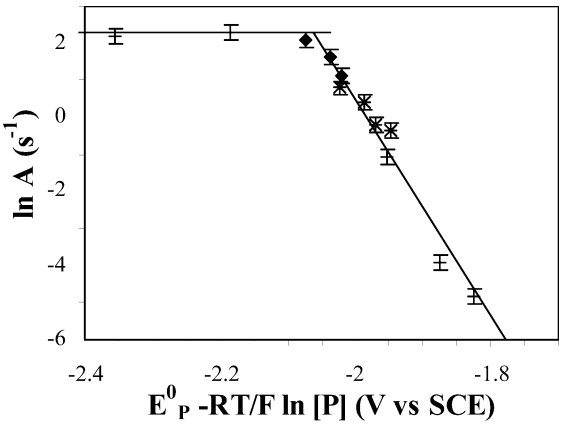

Figure 8. Nucleation of the PTFE carbonization process. Variation of the nucleation rate constant *A* with the driving force of the reduction process, $E_P^0 - RT/F \ln[P]$. Mediator concentration: 2−50 mM. The conditions are the same as those in Figure 1. From left to right: +, naphthalene, benzonitrile; ◆, 4-phenylpyridine; ∗, 2,2′-dipyridyl; +, phenanthridine, 2,4′-dipyridyl, anthracene.

is potential dependent. The potential dependence is introduced by assuming that the electrochemical driving force is related to the number of atoms, n_c, in the critical nucleus and the overpotential, η[47]

$$\delta\Delta G^{\neq}/\delta\Delta G^0 = (n_c + \alpha)F\eta \qquad (26)$$

According to this theory, a linear relationship between ln(*A*) and the driving force (here $\eta = -E_P^0 + \mathrm{RT/Fln[P]} + Cst$) is expected. From the slope of 26 V^{-1} obtained for (26), the value of $n_c + \alpha = 0.6_6$ was obtained, which suggests the atomic dimension of the critical nucleus.

The potential dependence of *B* is important for the three most positive redox mediators and less appreciable for the most negative ones. *B* depends on concentration according to $B \propto [P]^{0.4}$, which is close to the proposed square-root concentration dependency of $(\kappa_r')^{1/2}$. These arguments suggest that κ_r' and N_0 are potential independent at large driving force. Knowing κ_r', an estimate of the reduced sites density was deduced from the value of B and from a combination of (13), (18), and (21)

$$N_0 \approx \frac{3B}{\xi\kappa_h^{3/2}} \frac{D_s[P]}{2(2+\delta)\pi C_P d} \qquad (27)$$

If one considers that the diffusive vertical expansion at short and long time is the same, $\kappa_h^{1/2} = 3.7 \times 10^{-6}$ cm $s^{-1/2}$ (for [P] = 0.05 M), a value of $N_0 \sim 10^7$ cm^{-2} ensues. The latter is consistent with the number of 7×10^6 cm^{-2} obtained from the counting of the nuclei after a short potential pulse (25 s) at a 25 μm radius tip held at $d = 1.9$ *a* from the PTFE surface where P = 2,2′-dipyridyl. This agreement comforts our analysis of the short-time experiments.

At a lower driving force, κ_r' becomes potential dependent, which might invalidate the application of the diffusion-limited growth model for the three redox mediators with $E^0 > -2.0$ V vs SCE. However, the consideration of a growth kinetically limited by charge-transfer implies that $r_n(t) = k_{ct}t$ (k_{ct}, heterogeneous charge transfer rate constant) and finally leads to values of *A* and *B* not greatly different from those obtained by the diffusive controlled growth.

4. Conclusions

We have used SECM to locally reduce a PTFE surface. The reducing species was generated at a SECM tip at a close and constant distance from the PTFE surface. The observation of the current transients was analyzed in order to give more insight into the PTFE reduction process and to present general trends for local PTFE microfabrication.

At long time, the expansion of the PTFE carbonization proceeds in a hemi-ellipsoidal fashion, the radial expansion being much easier than the in-depth one. Those expansions were correlated to the tip current while changing different experimental variables such as the reduction time, the reducing species concentration, the nature of the electrolytic solution, the SECM tip radius, and the tip−substrate separation.

This study helped estimate the stoichiometry of the reduction reaction and confirmed the existence of two kinetic regimes owing to the redox mediator reduction potential. A rough model was proposed in which the reduction along the in-depth direction is mainly controlled by a diffusive process describing the transport of a reactive species into the reduced PTFE layer while, as already stated, the material resistivity controls the radial expansion. The observed variations may be explained by the penetration of the reducing species into the rough reduced PTFE material.

At shorter times, the PTFE phase transformation resembles a nucleation process and it has been analyzed in this respect. Even if the PTFE reduction is dependent on the heterogeneity of the sample surface, general trends were observed. The nucleation rate follows a potential dependency similar to that observed for other nucleation processes such as conducting polymer growth or metal deposition. Even though a simplified nucleation model was adopted, the SECM setup seems a promising tool for the quantitative investigation of phase transformation kinetics.

References and Notes

(1) Carlson, D. P.; Schmiegel, W. *Ullmann's Encyclopedia of Industrial Chemistry*, 5th ed.; Wiley: New York, 1988; Vol. A 11, pp 393−429.
(2) Gangal, S. V. *Encyclopedia of Polymer Science and Engineering*; Wiley: New York, 1989; Vol. 16.
(3) Allmer, K.; Feiring, A. E. *Macromolecules* **1991**, *24*, 5487.
(4) Said, M. A.; Balik, C. M.; Carlson, J. D. *J. Pol. Sci., Pol. Phys.* **1988**, *26*, 1457.
(5) Costello, C. A.; McCarthy, T. J. *Macromolecules* **1984**, *17*, 2940.
(6) Costello, C. A.; McCarthy, T. J. *Macromolecules* **1987**, *20*, 2819.
(7) Bening, R. C.; McCarthy, T. J. *Macromolecules* **1990**, *23*, 2648.
(8) Shoishet, M. S.; McCarthy, T. J. *Macromolecules* **1990**, *24*, 982.
(9) Iqbal, Z.; Ivory, D. M.; Szobota, J. S.; Elsenbauer, R. L.; Baughman, R. H. *Macromolecules* **1986**, *19*, 2992.
(10) Lukas, J.; Lochman, L.; Kalal, J. *Angew. Makromol. Chem.* **1990**, *181*, 183.
(11) Hung, M. H.; Burch, R. R. *J. Appl. Polym. Sci.* **1995**, *55*, 549.
(12) Chakrabarti, N.; Jacobus, J. *Macromolecules* **1988**, *21*, 3011.
(13) Combellas, C.; Richardson, S.; Shanahan, M. E. R.; Thiébault, A. *Int. J. Adhes. Adhes.* **2001**, *21*, 59.

(14) Brewis, D. M.; Dahm, R. H. *Int. J. Adhes. Adhes*. **2001**, *21*, 397.
(15) Kavan, L. In *Chemistry and Physics of Carbon*; Thrower, P. A., Ed.; Marcel Dekker: New York, 1991; Vol. 23, pp 71−171.
(16) Kavan, L. *Chem. Rev.* **1997**, *97*, 3061.
(17) Jansta, J.; Dousek, F. P. *Electrochim. Acta* **1973**, *18*, 673.
(18) Dousek, F. P.; Jansta, J. *Electrochim. Acta* **1975**, *20*, 1.
(19) Kavan, L.; Dousek, F. P.; Jansta, J. *Solid State Ionics* **1990**, *38*, 109.
(20) Dahm, R. H.; Barker, D. J.; Brewis, D. M.; Hoy, L. R. J. In *Adhesion*; Allen, K. W., Ed.; Applied Science Publ.: London, 1990; Vol. 4, pp 215−232.
(21) Barker, D. J.; Brewis, D. M.; Dahm, R. H.; Gribbin, J.; Hoy, L. R. J. *Electrochim. Acta* **1978**, *23*, 1107.
(22) Barker, D. J.; Brewis, D. M.; Dahm, R. H.; Hoy, L. R. J. *Polymer* **1978**, *19*, 856.
(23) Barker, D. J.; Brewis, D. M.; Dahm, R. H.; Hoy, L. R. J. *J. Mater. Sci.* **1979**, *14*, 749.
(24) Barker, D. J.; Brewis, D. M.; Dahm, R. H.; Gribbin, J.; Hoy, L. R. J. *J. Adhesion* **1981**, *13*, 67.
(25) Miller, M. L.; Postal, R. H.; Sawyer, P. N.; Martin, J. G.; Kaplit, M. J. *J. Appl. Polym. Sci.* **1970**, *14*, 257.
(26) Brecht, H.; Mayer, F.; Binder, H. *Angew. Makrom. Chem.* **1973**, *33*, 89.
(27) Brace, K.; Combellas, C.; Delamar, M.; Dujardin, E.; Kanoufi, F.; Shanahan, M. E. R.; Thiébault, A. *Polymer* **1997**, *38*, 3295.
(28) Benderly, A. A. *J. Appl. Polym. Sci.* **1962**, *6*, 221.
(29) Brewis, D. M.; Dahm, R. H.; Konieczko, M. B. *Angew. Makromol. Chem.* **1975**, *43*, 191.
(30) Amatore, C.; Combellas, C.; Kanoufi, F.; Sella, C.; Thiébault, A.; Thouin, L. *Chem. Eur. J.* **2000**, *6*, 820.
(31) Combellas, C.; Ghilane, J.; Kanoufi, F.; Mazouzi, D. *J. Phys. Chem. B* **2004**, *108*, 6391.
(32) Combellas, C.; Fuchs, A.; Kanoufi, F. *Anal. Chem.* **2004**, *76*, 3612.
(33) Costello, C. A.; McCarthy, T. J. *Macromol*. **1984**, 17, 2940.
(34) Brace, K.; Combellas, C.; Delamar, M.; Fritsch, A.; Kanoufi, F.; Shanahan, M. E. R.; Thiébault, A. *J. Chem. Soc, Chem. Commun.* **1996**, 403.
(35) Belzung, B.; Brace, K.; Combellas, C.; Delamar, M.; Kanoufi, F.; Shanahan, M. E. R.; Thiébault, A. *Polymer* **1998**, *39*, 4867.
(36) Wittman, J. C.; Smith, P. *Nature* **1991**, *352*, 414.
(37) Kanoufi, F.; Combellas, C.; Shanahan, M. E. R. *Langmuir* **2004**, *19*, 6711.
(38) Wei, C.; Bard, A. J.; Mirkin, M. V. *J. Phys. Chem.* **1995**, *95*, 16033.
(39) Mirkin, M. V. In *Scanning Electrochemical Microscopy*; Bard, A. J., Mirkin, M. V., Eds.; Marcel Dekker: New York, 2001; Chapter 5, p 145.

(40) In the present case, the use of eq 1 is arguable since such an equation was originally derived for a steady-state SECM process and an infinitely large substrate size, which is not always the case here since the size of the substrate is progressively increasing from zero. However, the validity of eq 1 should not be questioned at times longer than 25 s and for redox mediators such as $E° < -2.1$ V vs SCE since in this case the carbonized zone shows a radius larger than $2a = a + 1.5$d when $d = 0.68a$ (cf Figure 4). Conversely, for the same mediators, the question remains for the initial current rise and for the nucleation analysis. We have shown that the nucleation proceeded on a disk of a radius of approximately $2a$. Since the part of the signal that could be clearly analyzed typically starts at the half-value of the maximum current, this indicates that approximately half the area of this nucleating disk is electroactive, which corresponds to a disk of a radius of approximately $1.4a$. We believe that for such a surface area expression 1 is not too erroneous. The validation by numerical calculation is out of the scope of the present paper. We have started such numerical calculations and shown that eq 1 was still valid for conducting disks of a radius $> a$ held at $d = 0.68a$.

(41) Unwin, P. R.; Bard, A. J. *J. Phys. Chem.* **1991**, *95*, 7814−7824.
(42) Bard, A. J.; Mirkin, M. V.; Unwin, P. R.; Wipf, D. O. *J. Phys. Chem.* **1992**, *96*, 1861.
(43) Lexa, D.; Savéant, J.-M.; Shäfer H. J.; Su, K.-B.; Vering, B.; Wang, D. L. *J. Am. Chem. Soc.* **1990**, *112*, 6162 and references therein.
(44) Combellas, C.; Kanoufi, F.; Thiebault, A. *J. Phys. Chem. B* **2003**, *107*, 10894.

(45) (a) By definition,[45b] $i_{red} = \int\int_S \vec{j}\cdot d\vec{S}$, where S is the hemi-ellipsoid surface. Using spherical coordinates and projections of the current density, $\vec{j} = (j_r \cos\theta\ \vec{r} + j_h \sin\theta\ \vec{h})$ [$\vec{r}$ and $\vec{h}$ being unity vectors and $j_k = (2 + \delta)Fm_k$] along the radial, r, and vertical, h, directions, one obtains $i_{red} = \int j_r rh \cos^3\theta\ d\varphi\ d\theta + \int j_h r^2 \cos\theta \sin^2\theta\ d\varphi\ d\theta = i_r + i_h$. After integration along the external surface of the hemi-ellipsoid and using average current densities $\langle j_r\rangle$ and $\langle j_h\rangle$ along respectively the vertical and radial directions of respective lengths h_{red} and r_{red}, one obtains $i_{red} = 2\pi/3\langle j_r\rangle r_{red}h_{red} + \pi/3\langle j_h\rangle r_{red}^2$. (b) *Electrochemical Methods: Fundamentals and Applications*, 2nd ed.; Bard, A. J., Faulkner, L. R., Eds.; Wiley: New York, 2001; Chapters 3 and 4, pp 87−136.

(46) $\langle m_h\rangle = D_r\nabla C_r$ can be approximated by D_rC_r/h_r, if one assumes that the reduced species that ensures the diffusive control diffuses from the liquid-polymer interface to the polymer-virgin PTFE interface.[45b]

(47) Budevski, E. B. In *Comprehensive Treatise of Electrochemistry*; Conway, B. E., Bockris, J. O'M., Yeager, E., Khan, S. U., White, R., Eds.; Plenum Press: New York, 1983; Vol 7, p 399.
(48) Correia, A. N.; Machado, S. S. S.; Sampaio, J. C. V.; Avaca, L. A. *J. Electroanal. Chem.* **1996**, *107*, 37.
(49) Heerman, L.; Tarallo, A. *J. Electroanal. Chem.* **1998**, *451*, 101.
(50) Cao, Y.; West, A. C. *J. Electroanal. Chem.* **2001**, *514*, 103.
(51) For a review see for example: Hyde, M. E.; Compton, R. G. *J. Electroanal. Chem.* **2003**, *549*, 1.
(52) Hyde, M. E.; Klymenko, O. V.; Compton, R. G. *J. Electroanal. Chem.* **2002**, *534*, 13.
(53) Sluyters-Rehbach, M.; Wijenberg, J. H. O. J.; Bosco, E.; Sluyters, J. H. *J. Electroanal. Chem.* **1987**, *236*, 1.
(54) Heerman, L.; Tarallo, A. *J. Electroanal. Chem.* **1999**, *470*, 70.
(55) Avrami, M. *J. Chem. Phys.* **1939**, *7*, 1103.
(56) Avrami, M. *J. Chem. Phys.* **1940**, *8*, 212.